Carbohydrate Polymers 97 (2013) 421–428

Contents lists available at SciVerse ScienceDirect

Carbohydrate Polymers

journal homepage: www.elsevier.com/locate/carbpol

Synthesis and characterization of pullulan-mediated silver nanoparticles and its antimicrobial activities

Paulraj Kanmani, Seung Taik Lim*

School of Life Sciences and Biotechnology, Korea University, 5-1 Anam-dong, Sungbuk-ku, Seoul 136-701, South Korea

ARTICLE INFO

Article history:
Received 11 February 2013
Received in revised form 11 April 2013
Accepted 12 April 2013
Available online 6 May 2013

Keywords:
Pullulan
Silver nanoparticles
Antibacterial
Antifungal
Antibiofilm

ABSTRACT

Synthesis of silver nanoparticles was achieved using pullulan as both a reducing and stabilizing agent. The effect of pullulan and silver nitrate amounts on the synthesis of silver nanoparticles (AgNPs) was investigated. The formation of nanoparticles was first screened by measuring the surface plasmon resonance peak at 420–430 nm using UV–vis spectroscopy. The morphology of the synthesized AgNPs was determined using TEM, which indicated that the AgNPs varied in shape and polydispersed with an average size of 2–30 nm. The presence of elemental silver and the crystalline structure of the AgNPs were confirmed by EDX and XRD analyses. The possible functional groups of pullulan responsible for the reduction and stabilization of AgNPs were evaluated using FT-IR. The pullulan-reduced AgNPs showed excellent antibacterial, antifungal, and antibiofilm activity against food and multidrug resistant bacterial and fungal pathogens. The results showed that pullulan could be used as a reducing as well as a capping agent for synthesizing AgNPs which had potent antimicrobial activity.

1. Introduction

For the last decades, nanotechnology is a skyrocketing multidisciplinary field of research that interweaves physics, chemistry, bionanoscience, and materials science. Recently, nanobiotechnology is being becoming as an emerging and remarkable technology for the production of novel functional materials such as nano-sized particles. Nanoparticles (NPs) have been widely used in various real world industrial, biomedical, and scientific applications. Nowadays, several types of metal nanoparticles (MNPs) such as gold, silver, zinc, and copper have been successfully synthesized with various anticipated applications that includes medicine and diagnosis, nutrition and neutraceuticals, and electronics and optics (Duncan, 2011; Sharma, Yngard, & Lin, 2009). Among them, silver nanoparticles (AgNPs) have attracted special attention because of their widespread physical, chemical, and biological nature, unique particle size (<100 nm), and tunable surface plasmon resonance (Sharma et al., 2009). Various physical and chemical methods have been utilized for the production of silver, gold, and other nanoparticles successfully (Bankura et al., 2012; Wei et al., 2012). Most commonly, chemical reduction methods are being used by researchers for the production nanoscale metal particles.

Chemical reducing agents such as sodium borohydride (Moura, Mattoso, & Zucolotto, 2012), trisodium citrate (Hebeish, Hashem, Abd El-Hady, & Sharaf, 2013), sodium hydroxide (Bankura et al., 2012), N,N-dimethyl formamide (Guari et al., 2003), 2-mercaptobenzimidazole (Stiger, Gorer, Craft, & Penner, 1999), sodium dodecyl sulfate (Kora & Arunachalam, 2011), *etc.*, have been employed for the production and stabilization of NPs and also found to show certain toxicological effects in the medical research field. Some other methods such as gamma ray and solar irradiation (Wei et al., 2012; Yoksan & Chirachanchai, 2010), sono chemical deposition (Pol et al., 2002), electrochemical methods (Zhu, Liu, Palchik, Kottypin, & Gedanken, 2000), UV photo reduction (Kora & Arunachalam, 2011) and microwave assisted (Peng, Yang, & Xiong, 2013) have also been utilized for synthesis of NPs. However, those reducing agents and physical processes are quite expensive and hazardous. Thus, stupendous efforts are being made to fabricate AgNPs using eco-friendly, biocompatible, and safe biological resources or processes. Biological materials such as bacteria, fungus, yeasts, plant extracts, actinomycetes, and some biomolecules have been stated as safe to synthesize of MNPs on extracellular and intercellular level (Bankura et al., 2012; Narayanan & Sakthivel, 2011). Some studies have reported on extracellular and intracellular synthesis of MNPs using the fungi *Cylindrocladium floridanum* (Narayanan & Sakthivel, 2011); *Alternaria alternate* (Gajbhiye, Kesharwani, Ingle, Gade, & Rai, 2009); bacteria such as *Bacillus amyloliquefaciens* (Wei et al., 2012) and *Bacillus licheniformis* (Kalishwaralal, BarathManiKanth, Ram Kumar Pandian, Deepak, & Gurunathan, 2010); and plants such as plant *Hibiscus cannabinus* (Bindhu & Umadevi, 2013) and *Cocos nucifera* coir extract (Roopan et al., 2013).

* Corresponding author. Tel.: +82 2 3290 3435; fax: +82 2 921 0557.
E-mail address: limst@korea.ac.kr (S.T. Lim).

0144-8617/$ – see front matter © 2013 Elsevier Ltd. All rights reserved.
http://dx.doi.org/10.1016/j.carbpol.2013.04.048

Recently, there is a growing interest in the fabrication of novel AgNPs with potent antimicrobial nature and new functional attributes using polysaccharides such as chitosan (Yoksan & Chirachanchai, 2010), starch (Mohanty et al., 2012), agar (Shukla, Singh, Reddy, & Jha, 2012), dextran (Bankura et al., 2012), hydrolyzed casein (Radzig et al., 2013), and guar gum (Pandey, Goswami, & Nanda, 2012). However, there is no report on microbial polysaccharide such as pullulan as a reducing and stabilizing agent for the production of metal nanoparticles. Pullulan is a microbial linear homopolysaccharide consisting of repeating units of glucose that is often termed a biopolymer of α-1, 6 glycosidic linked maltotriose units (Mona & Ajay Kumar, 2004; Wu, Zhong, Li, Shoemaker, & Xia, 2013). Pullulan is highly water soluble and is synthesized extracellularly by the polymorphic fungus *Aureobasidium pullulans*. It has various potential applications especially in the food and pharmaceutical industries. Due to its outstanding adhesive and film forming properties, pullulan has been used to make compression moldings, fibers, drug delivery carrier materials, and edible film (Mona & Ajay Kumar, 2004; Wu et al., 2013).

In the present study, the synthesis of pullulan-mediated AgNPs by direct reduction of silver nitrate with pullulan was demonstrated. The synthesized AgNPs were characterized using UV–vis spectroscopy, transmission electron microscopy (TEM), energy-dispersive X-ray spectroscopy (EDX), dynamic light scattering (DLS), X-ray diffraction (XRD), and Fourier transform infrared (FT-IR) spectroscopy. In addition, the antibacterial, antifungal and antibiofilm activity of the pullulan-stabilized AgNPs *in vitro* will be examined.

2. Materials and methods

2.1. Materials and microbial strains

Biopolymer pullulan was procured from Putus Macromolecular Sci & Tech. Ltd. (Wuhan, China). Silver nitrate, brain heart infusion broth (BHIB), tryptic soy broth (TSB), potato dextrose agar (PDA), nutrient broth (NB), Muller–Hinton agar, and agar powder were purchased from Duksan Pure Chemicals Co., Ltd. (Gyeonggido, South Korea). Bacterial strains such as *Escherichia coli* ATCC 35218, *Bacillus cereus* ATCC 10987, food borne pathogen *Listeria monocytogenes* ATCC 15313, and the multidrug resistant pathogens *Pseudomonas aeruginosa* ATCC 15442 and *Klebsiella pneumonia* ATCC 27736 were obtained from the Korean Collection for Type Cultures (KCTC) in South Korea. Fungal pathogens such as *Aspergillus* spp. and *Penicillium* spp. were isolated from contaminated food and subsequently characterized in our laboratory. All solutions were made using ultra-filtered high purity deionized water.

2.2. Preparation of pullulan-based silver nanoparticles (AgNPs)

Various concentrations of pullulan (1%, 5%, 10%, and 15%) were mixed with a 9 mM aqueous solution of silver nitrate ($AgNO_3$) prepared freshly in deionized water under magnetic stirring to optimize the pullulan concentration for $AgNO_3$ synthesis. Different concentrations of $AgNO_3$ (1, 3, 5, 7, 9, and 12 mM) in 15% of pullulan solution were compared under the same conditions. Subsequently, the homogeneous solutions were autoclaved at 121 °C for 15 min. The viscous white-colored solutions turned yellow, which confirmed the formation of pullulan-based AgNPs. All solutions were stored at room temperature (22–25 °C) for more than 3 months in a dark place.

2.3. Characterization of AgNPs

The biopolymer reduction of Ag^+ ions in the aqueous solutions were monitored by measuring the ultraviolet–visible absorbance spectrum of the solution using a UV-vis spectrophotometer (BIOMATE-3S, Thermo Fisher Scientific, Boston, MA, USA) in the range of 300–700 nm. For the analysis of TEM, a drop of AgNPs containing aqueous solution was directly placed onto a carbon-coated copper grid and allowed to air dry completely prior to the TEM observations. The TEM images of AgNPs were obtained using a transmission electron microscope (FEI Tecnai G2 F30, Eindhoven, The Netherlands) at an accelerating voltage of 300 kV. EDX analysis was also carried out using the same TEM equipment to confirm the elemental silver present in the NPs. The size of the AgNPs was evaluated using the DLS method (Wyatt Technology Corp, Santa Barbara, CA, USA), which uses laser light diffraction to measure particle size distribution. The phase composition and crystal structure of the AgNPs was determined with XRD (Philips XPERT MPD). A dried sample was prepared by placing it on a microscopic glass slide and the diffractogram was recorded using Cu-Kα radiation and a nickel monochromator filtering wave at a voltage and current of 40 kV and 30 mA, respectively. The FT-IR spectrum of the pullulan-stabilized AgNPs were analyzed using FT-IR spectroscopy (JASCO FT-IR 460, Daejon, South Korea) operated at a resolution of 4 cm^{-1}. The dried sample was powdered by grinding with KBr pellets and pressed into a mold. The spectrum was recorded between the wavelength ranges of 500–4000 cm^{-1}.

2.4. Antibacterial activity of AgNPs

The antibacterial activity of the pullulan-stabilized AgNPs was measured using the agar well diffusion method. Bacterial pathogens such as *E. coli*, *K. pneumonia*, *P. aeruginosa*, and *L. monocytogenes* were used as indicator strains for this analysis. These bacterial strains were aseptically inoculated into tryptic soy broth (TSB) and brain heart infusion broth (BHIB) broth, and then incubated at 37 °C. After 16 h, the cells (1 ml) were centrifuged at 6000 rpm for 10 min and then the cells were suspended in sterile water (2 ml). Cells from different pathogens (1 ml) were added to tryptic soy agar (TSA) and brain heart infusion agar (BHIA) media (100 ml) prior to plating and wells were made using an agar well borer. Different concentrations of AgNPs (80 μl) were added to these wells, and the plates were incubated at 37 °C for 24 h. Zone of inhibitions were estimated by measuring the diameter of the bacterial growth inhibition zone. The values were averaged from three independent experiments.

Moreover, the antibacterial activity of the AgNPs was analyzed in liquid medium using the plate count method. To this experiment, the cells of various bacterial pathogens (10^6 CFU/ml) were taken in separate Eppendorf tubes containing various concentrations of AgNPs and then incubated at 37 °C for 6 h. At desired time intervals, the relative cell viabilities of various pathogens were estimated by counting bacterial colonies on the plates. Pure pullulan and silver nitrate solutions were used as controls for comparison. All experiments were carried out in triplicate.

2.5. Antifungal activity of AgNPs

The antifungal activity of the AgNPs was measured using the agar well diffusion method. Two fungal pathogens were isolated from contaminated food and identified as *Aspergillus* spp. and *Penicillum* spp. These two fungal strains were inoculated in potato dextrose agar medium (PDA) and incubated at room temperature (25–27 °C) for 4 days. Four day old fungal spores were collected by washing with water and subsequently plated (0.1 ml) on PDA plate. Wells were made using an agar well borer. Various concentrations of AgNPs were added to the wells and incubated at room temperature for 4 days. Zone of inhibitions were estimated by measuring

the diameter of the fungal growth inhibition zone. The values were averaged from three independent experiments.

2.6. Evaluation of K^+ ions efflux from bacterial strains

The mechanistic action of the pullulan-reduced AgNPs was estimated by measuring efflux of K^+ ions from various bacterial pathogens into the surrounding medium. For this experiment, food borne and multidrug resistant pathogens such as *E. coli*, *K. pneumonia*, *P. aeruginosa*, and *L. monocytogenes* were cultured in TSB and BHIB at 37 °C. After 16 h, the cells were centrifuged at 6000 rpm for 10 min and then serially diluted to two-fold. AgNPs (100 μg/ml) were mixed with different bacterial strains and subsequently incubated at 37 °C for 2 h and centrifuged at 6000 rpm for 10 min to remove the cell debris. Water/AgNPs and water/each bacterial strain served as controls. The leakage of K^+ ions from the cells was measured using inductively coupled plasma-optical emission spectroscopy (ICP-OES, JY Ultima 2C, Jobin Yvon, France).

2.7. Effect of antibiofilm activity of pullulan stabilized AgNPs

Bacterial pathogens such as *E. coli*, *B. cereus*, *L. monocytogenes*, and *P. aeruginosa* were inoculated into TSB and BHIB, and incubated at 37 °C for 16 h. The cultures were serially diluted 1:100 in fresh liquid medium containing various concentrations of AgNPs and subsequently incubated at 37 °C for 24 h under gentle shaking (100 rpm). Polystyrene microtiter plates (96 wells) were used for the growth of bacterial pathogens. Unattached cells were removed using pipette, and the wells were washed twice with sterile water. The attached cells were stained with 0.1% crystal violet. After a 10 min staining period, the crystal violet was removed and the wells were thoroughly washed twice with sterile water. The cells associated with the crystal violet were solubilized with absolute ethanol and the absorbance was recorded at 600 nm to quantify antibiofilm activity of the AgNPs. These experiments were repeated three times with six replicates, and average values were calculated.

3. Results and discussion

3.1. UV–vis spectrophotometer

Silver nanoparticles were synthesized by the reduction of Ag^+ into Ag^0 with the addition of pullulan into various concentrations of silver nitrate followed by heating at 121 °C. The colorless solutions turned yellowish brown indicating the formation of AgNPs. The effect of different concentrations of pullulan and silver nitrate on the production of AgNPs was investigated and their spectra are shown in Fig. 1. It seemed that the AgNPs absorbed radiation in the visible regions of 400–450 nm due to the strong SPR transition. The appearance of the SPR transition in this region confirmed the production of AgNPs (Bankura et al., 2012; Pandey et al., 2012). Fig. 1a predicts the UV–vis spectra of the AgNPs obtained by addition of different concentrations of pullulan into the silver nitrate solution. The results showed that the UV–vis spectra of the AgNPs could depend on the pullulan concentration. Substantial increase in SPR bands were observed with increasing addition of pullulan into the silver nitrate solution. It was clear that pullulan concentration played a significant role in the formation and stabilization of the AgNPs. Similarly, a gradual increase in absorption intensity was observed when the concentration of the guar gum (GG) was increased from 1.2% to 3.5% (Pandey et al., 2012). The higher concentration of GG could be attributed to enhanced stabilization of the synthesized AgNPs. Factors such as temperature, pH, dielectric properties, and size and shape of particles determine the absorbance and position of the SPR bands (Gan, Ng, Huang, & Yau Li, 2012). Moreover, the concentrations of silver nitrate play a role

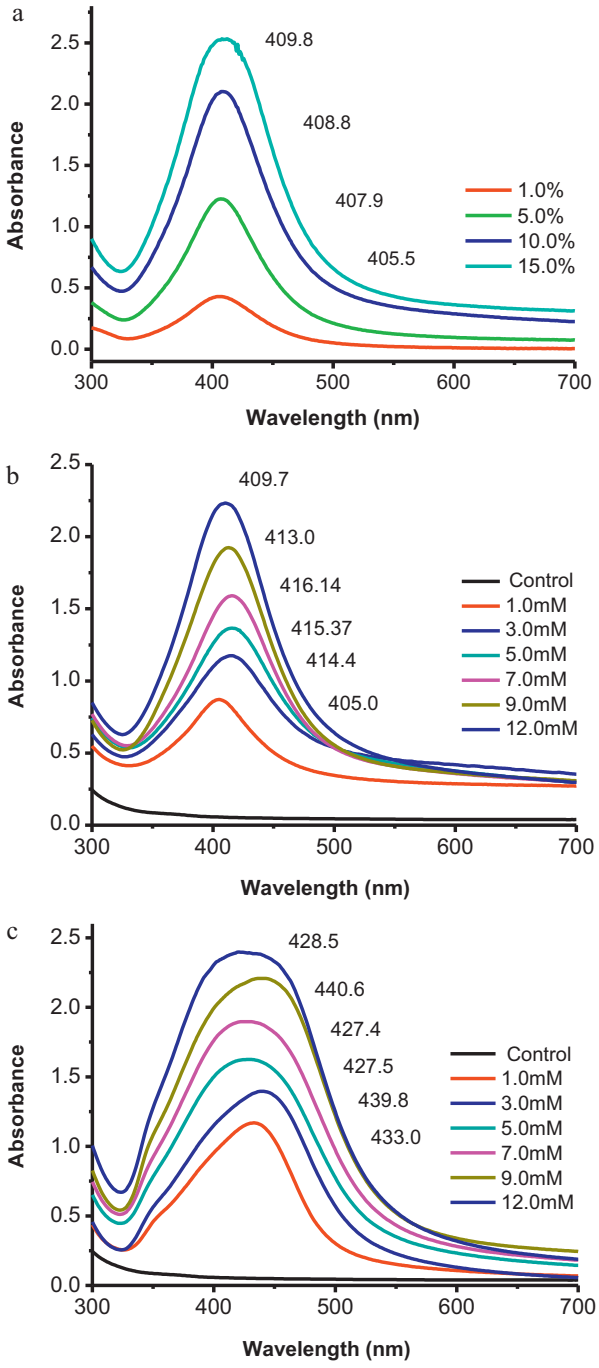

Fig. 1. UV–vis spectra of peaks produced by silver nanoparticles at different concentrations of pullulan (a), silver nitrate (b) and after 3 months storage (c) at room temperature.

in the formation of AgNPs as shown in Fig. 1b. The increased concentration of silver nitrate added to the pullulan solution resulted in a substantial increase in the SPR bands. The maximum absorption peak was observed by adding 12 mM $AgNO_3$. In contrast, no absorption band was observed in the control pullulan alone. A similar result was observed by Pandey et al. (2012) who found that the UV–vis absorption spectra of the guar gum stabilized AgNPs increases as the silver nitrate concentration is increased from 2.5 to 15 mM. In addition, UV–vis spectra of the same pullulan-stabilized AgNPs were recorded after 3 months storage at room temperature (Fig. 1c). As a result, the symmetric and very narrow SPR bands became slightly broader and the absorptions maxima shifted to

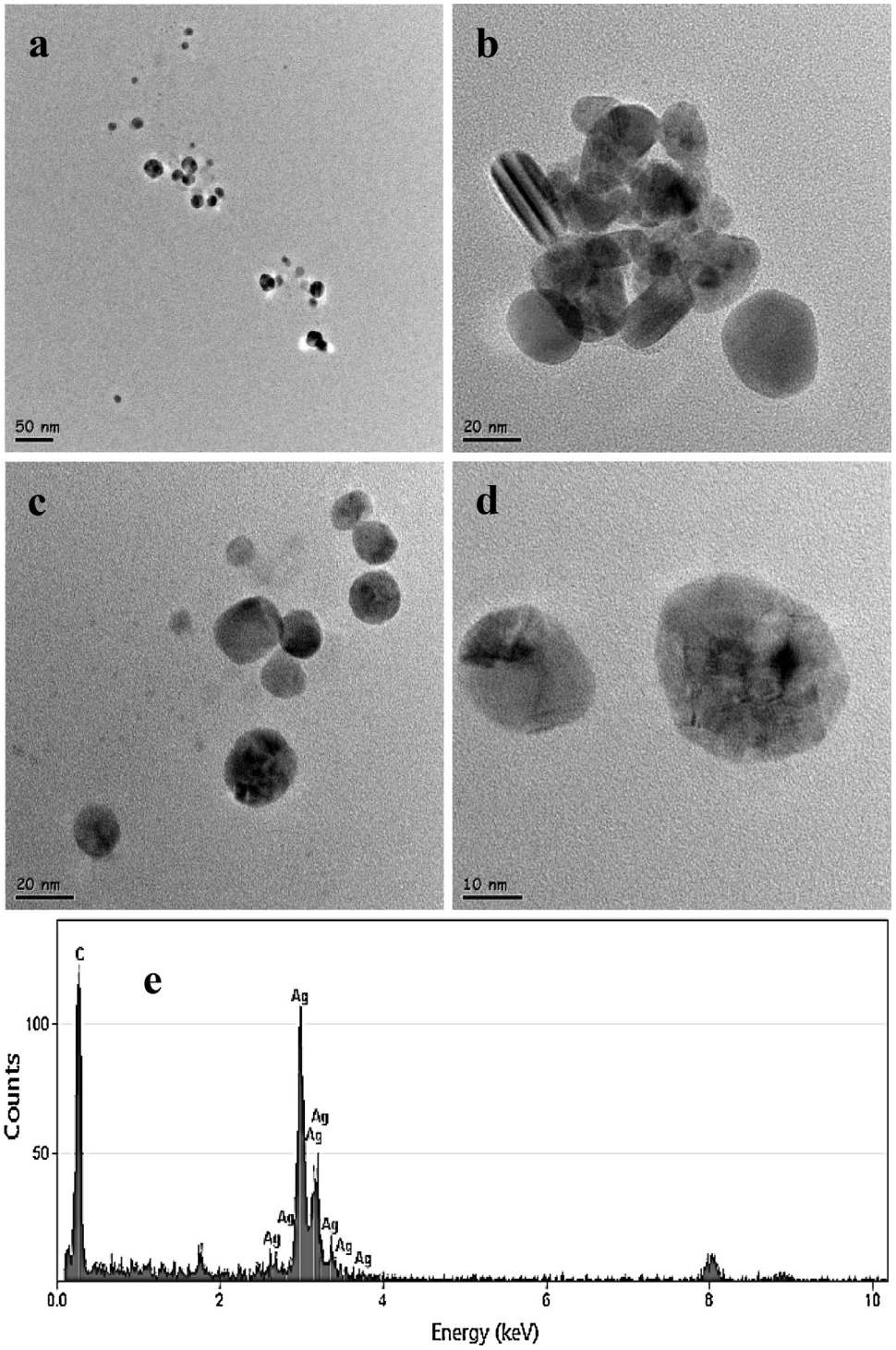

Fig. 2. TEM micrograph of pullulan reduced AgNPs at different magnifications (a)–(d) and EDX spectrum of AgNPs (e).

slightly different positions. These small changes in the AgNP UV–vis spectra suggested that the AgNPs were well capped by pullulan materials and that there was no agglomeration of the AgNPs. These results are in good agreement with those of Bankura et al. (2012) who found that the absorption maxima of dextran-stabilized AgNPs shifted to 425 nm after 30 days of storage. Bindhu and Umadevi (2013) reported that the increase in addition of sliver nitrate could induce the broadening and shifting the SPR band from 445 nm to 458 nm. These possible changes in the SPR band depend on particle size, shape, state of aggregation, and dielectric medium (Bindhu & Umadevi, 2013).

3.2. Morphological and structural characterization of pullulan-stabilized AgNPs

The size, shape, morphology and distribution of the pullulan-stabilized AgNPs were further confirmed with help of TEM and the results are shown in Fig. 2. Fig. 2b shows the AgNPs with rod and hexagonal shaped structures in which individual spherical and oval-shaped AgNPs with an average diameter of 2–40 nm were capped by pullulan molecules (Fig. 2c and d). Bankura et al. (2012) reported that the dextran-stabilized AgNPs are spherical in shape and have a size of 5–10 nm. The analysis of energy dispersive X-ray

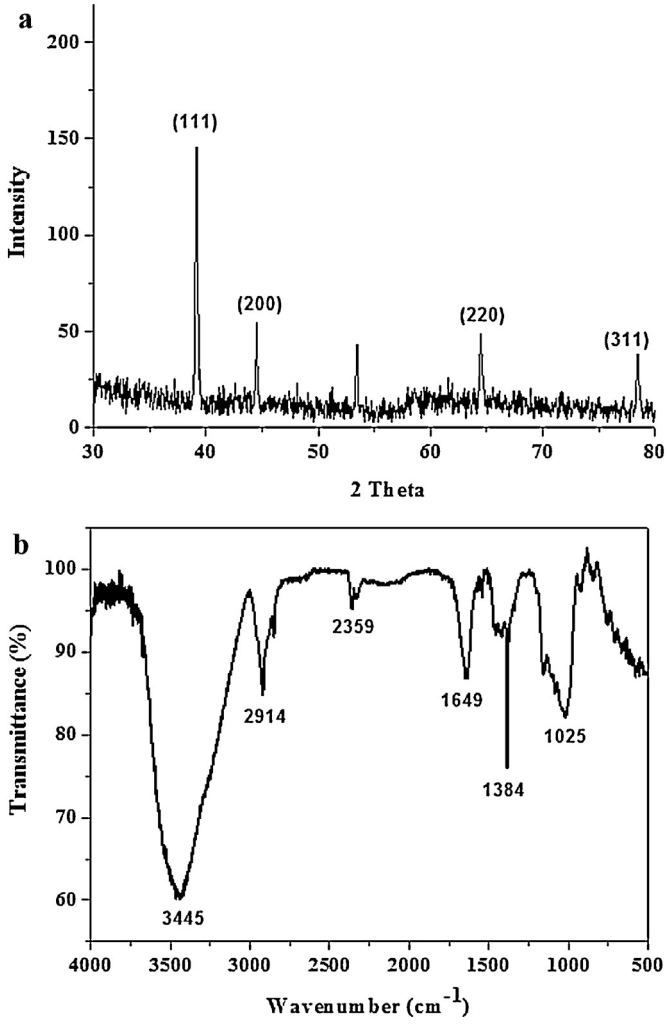

Fig. 3. X-ray diffraction pattern (a) and FT-IR spectrum (b) of the pullulan stabilized silver nanoparticles.

(XRD) spectroscopy provides the quantitative and qualitative status of the elemental silver involved in the formation of AgNPs (Bindhu & Umadevi, 2013). Fig. 2e shows the EDX spectrum of the pullulan-stabilized AgNPs. The strongest peak was revealed at ~3 keV, which confirmed the presence of elemental silver in the nanoparticles. Silver nanoparticles typically revealing optical absorption signals at ~3 keV could be due to the strong SPR (Magudapatty, Gangopaghyayrans, Panigrahi, Nair, & Dhara, 2001). Moreover, the atoms of O and N were detected with relatively very less intensity, whereas the C atom showed relatively similar intensity of elemental Ag. Similarly, Bankura et al. (2012) reported that the dextran-stabilized AgNPs exhibited strong signals in the silver region at ~3 keV. Furthermore, the EDX pattern of the carboxymethyl cellulose (CMC)-stabilizing AgNPs consists of Ag, O, and C with percentages of 18.99%, 47.54%, and 33.47% (Hebeish et al., 2013). The particles size distribution was analyzed using dynamic light scattering (DLS) analyzer. The particles were multimodal polydispersed which indicating a heterogeneous particles distribution with sizes of 5.6–97.6 nm (data not shown). This result differed from the results obtained by visual measurements using TEM. In contrast, Mohanty et al. (2012) reported that the starch-stabilized AgNPs are monodispersed with an average size of about 20 nm.

The crystalline nature of the pullulan-stabilized AgNPs was also confirmed by analysis of the XRD pattern. Fig. 3a shows the XRD pattern of the AgNPs with four distinctive diffraction peaks at 38.8, 44.5, 64.5, and 78.1 in the 2 theta region, which corresponded to (1 1 1), (2 0 0), (2 2 0), and (3 1 1) planes of silver. These typical XRD peaks indicate the presence of a face centered cubic (fcc) structure of crystalline AgNPs (Pandey et al., 2012; Peng et al., 2013). Among the corresponding planes, plane (1 1 1) was more intense compared to that of the other planes, which may have been due to the predominant orientation of the (1 1 1) plane. Moreover, an unidentified peak was observed with the Bragg peaks representative of fcc silver nanocrystals. The appearance of this sharp peak could have resulted from crystallization of the reducing and stabilizing agent in the AgNPs. Similar results were observed by Bankura et al. (2012) and Roopan et al. (2013) for AgNPs synthesized with dextran and a coir waste extract. An FT-IR spectrum measurement was also carried out to examine the possible functional groups of pullulan responsible for reduction and stabilization of the AgNPs. Fig. 3b shows the FT-IR spectrum of the pullulan-reduced AgNPs. It seems that the pullulan-reduced AgNPs revealed various characteristic peaks with ranges from 3345 cm^{-1} to 1025 cm^{-1}. A broad and strong absorption peak was observed at 3345 cm^{-1}, indicating the stretching vibration of the hydroxyl groups (O—H). In contrast, Jung, Jeong, and Kim (2003) found that the hydroxyl (O—H) and C—H stretching frequency of pure pullulan exhibits distinct peaks at 3356 cm^{-1} and 2943 cm^{-1}. The intense absorption peak at 2914 cm^{-1} corresponded to C-H stretching frequency. Moreover, the absorption peak at 1649 cm^{-1} indicated the presence of the carbonyl (C═O) stretching frequency. The peak at 1025 cm^{-1} may have been due to vibration of the O-H stretching. An additional absorption peak at 1384 cm^{-1} was influenced by the presence of AgNPs. All peaks observed in the FT-IR spectrum of pullulan-stabilized AgNPs differed from the FT-IR spectrum results for pure pullulan (Jung et al., 2003). These observations suggest a strong interaction of Ag with the pullulan functional groups. In addition, no new peak was observed in the FT-IR spectrum, suggesting that no new bond formation occurred between the pullulan and AgNPs. Pandey et al. (2012) reported that the O-H group of polymer had efficient coordination ability with silver ions.

3.3. Antimicrobial activity of AgNPs

The antibacterial activity of the AgNPs was investigated against food-born and multidrug resistant pathogens using the agar well diffusion and colony count methods. The results for the inhibitions zone and their average values are shown in Fig. 4a and c. It was apparent that all bacterial pathogens were highly inhibited in a dose-dependent manner. Increases in the inhibition zones were observed with an increase in the amount of AgNPs added. Among the bacterial pathogens, *P. aeruginosa* was more susceptible to AgNPs followed by *K. pneumonia* and *E. coli*. The food-born pathogen *L. monocytogenes* was less susceptible to the AgNPs. Overall, the Gram negative bacterial pathogens were highly suppressed by the AgNPs compared to Gram positive bacterial pathogens. Similarly, Priyadarshini, Gopinath, Meera Priyadharsshini, MubarakAli, and Velusamy (2013) reported that the Gram negative bacterium *E. coli* shows a maximum inhibition zone compared to that of the Gram positive bacteria *B. cereus* and *Streptococcus pyogenes*, which was probably due to the thick cell wall of bacteria. Gram positive bacterial strains are generally composed of a three-dimensional thick peptidoglycan (PG ~20–80 nm) layer compared to that of Gram negative bacteria (~7–8 nm). The PG layer possesses linear polysaccharide chains cross linked by more short peptides and thus forms a complex structure which makes it difficult for AgNPs to penetrate Gram positive bacteria (Priyadarshini et al., 2013). Bankura et al. (2012) reported that dextran-stabilized AgNPs (200 μg/ml) exhibit efficient antimicrobial activity against *Bacillus subtilis*, *B. cereus*, *E. coli*, and *P. aeruginosa* with inhibition zone diameters of 32, 28, 21, and 24 mm, respectively. Moreover, Shukla et al. (2012)

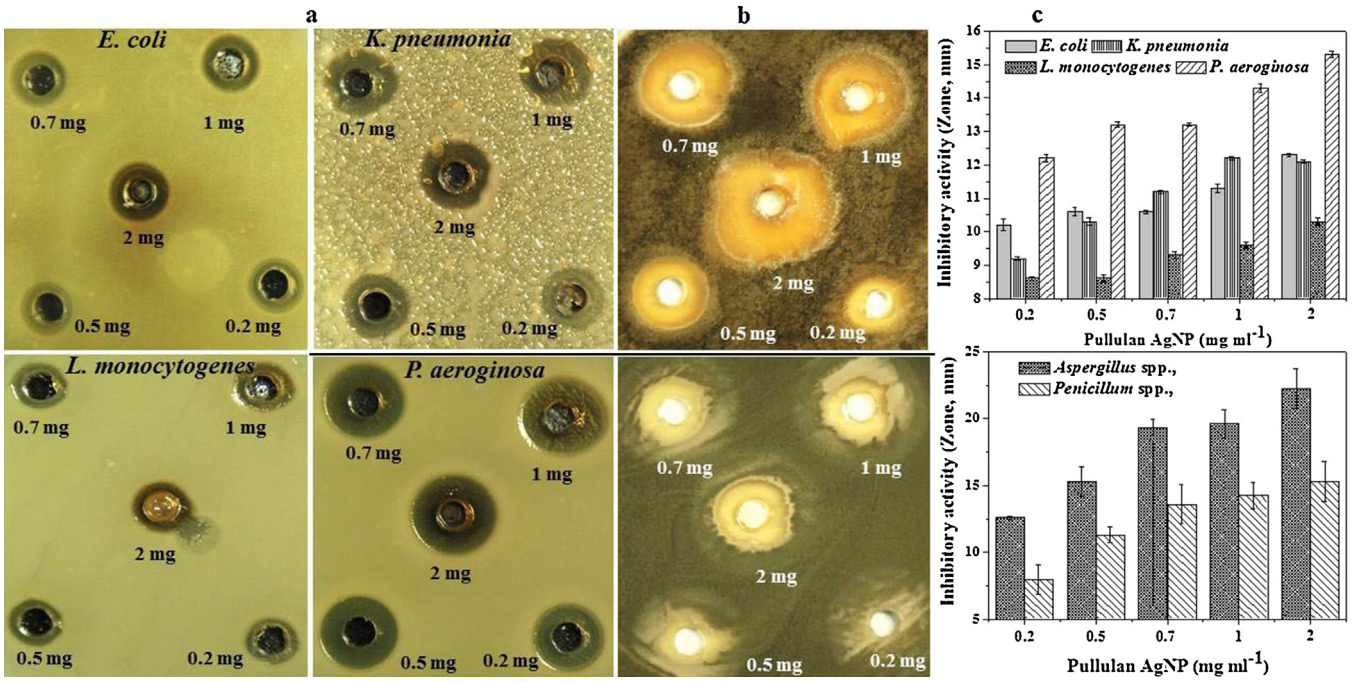

Fig. 4. Antimicrobial activity of different concentrations of AgNPs against the bacterial pathogens (a) (*E. coli*, *K. pneumonia*, *L. monocytogenes* and *P. aeruginosa*) and fungal pathogens (b) (*Aspergillus* spp. and *Penicillum* spp.) in agar medium after 24 h of incubation at 37 °C. (c) and (d) Average diameter inhibition zones of bacterial and fungal strains.

evaluated the antibacterial activity of agar-stabilized AgNPs against *Bacillus pumilus* using the disk diffusion method. The clear inhibition zone (24 mm) was observed after 24 h incubation at 37 °C. The antifungal activity of the AgNPs was analyzed using the agar well diffusion method. Fig. 4b and d shows the antifungal activity of the pullulan-stabilized AgNPs. *Aspergillus* spp. and *Penicillium* spp. were also inhibited in a concentration dependent manner. The radial growth inhibition zones increased when the concentration of AgNPs was increased from 1 to 5 mg/ml. The fungus *Aspergillus* spp. was more susceptible to the AgNPs.

The antibacterial activity of AgNPs was investigated also in liquid medium. For this, various concentrations of AgNPs were incubated with cells of different bacterial pathogens in liquid medium. The relative cell viabilities of various bacterial pathogens after 2 and 6 h of incubation at 37 °C were calculated (Fig. 5). In all cases, a substantial decrease in relative cell viability was observed after 2 and 6 h of incubation. Among them, more than 50% and 70% of cell deaths were observed at 70 μg/ml and 100 μg/ml concentrations in *P. aeruginosa* after 2 h of incubation at 37 °C, respectively, whereas after 6 h incubation no cell viability was observed. Moreover, the lower concentration (10 μg/ml) of AgNPs resulted in >50% cell death of *P. aeruginosa* after 6 h of incubation. As can be seen in Fig. 5c, the cells of *L. monocytogenes* were also killed by nearly 80% at 100 μg/ml after 6 h incubation. In contrast, the control $AgNO_3$ showed relatively higher cell viability due to the lower growth inhibition of the bacterial pathogens. These results are in good agreement with those of Mohanty et al. (2012) who found that starch-stabilized AgNPs had efficient antimicrobial activity against *Staphylococcus aureus*, *P. aeruginosa*, *Shigella flexneri*, and *Salmonella typhi*. All of these bacterial strains were inhibited in a dose dependant manner. More than 98% of the bacterial cell population was killed at 2 μM concentration of AgNPs after 4 h incubation. Shukla et al. (2012) also evaluated the antibacterial activity of agar-stabilized AgNPs against *B. pumilus* using a bacterial cell killing kinetic assay. The presence of AgNPs (500 μM) was significantly reduced the cell viability of *B. pumilus* (5×10^4 CFU/ml) compared to control (80×10^7 CFU/ml) after 24 h incubation period.

3.4. Induction of intracellular potassium efflux by AgNPs

Pore formation and disruption of the bacterial cell membrane are the most important mechanistic actions of AgNPs. The leakage of intracellular materials from cells could be induced by the above said action of AgNPs (Lok et al., 2006). Therefore, the massive leakage of potassium ions from bacterial pathogens due to the action of the pullulan-stabilized AgNPs was evaluated using ICP-OES and the results are shown in Table 1. The control (water/AgNPs) and control (water/different bacterial cells) showed lower values than those obtained for the test samples (bacterial cells/AgNPs). For assessing the amount of K^+ ions released from the cells due to the action of AgNPs alone, the values (ppm) of test samples were subtracted with results of control samples (a and b). After subtraction, maximum amount of K^+ ions efflux was observed in *P. aeruginosa* (670 ppm) followed by *K. pneumonia* (563 ppm), and *E. coli* (424 ppm) due to the action of AgNPs alone (Table 1). These results confirmed that the pullulan-stabilized AgNPs induced efflux of K^+ ions from the cells, which was probably due to pore formation or increased membrane permeability. Moreover, the release of K^+ ions during the exposure of cells into the silver nanoparticles suggests that the strong

Table 1
Effect of silver nanoparticles on the efflux of K^+ from the cells of bacterial pathogens.

Samples	K^+ conc (ppm) in liquid medium	Efflux of K^+ due to AgNPs (ppm)[c−(a+b)]
[a]Water/AgNPs (100 μg/ml)	74	
[b]Water/*E. coli* cells	145	
[b]Water/*K. pneumonia* cells	141	
[b]Water/*L. monocytogenes* cells	138	
[b]Water/*P. aeroginosa* cells	139	
[c]*E. coli*/AgNPs	643	+424
[c]*K. pneumonia*/AgNPs	778	+563
[c]*L. monocytogenes*/AgNPs	357	+145
[c]*P. aeruginosa*/AgNPs	883	+670

[a] Control (water/AgNPs).
[b] Control (water/different bacterial cells).
[c] Test samples (bacterial cells/AgNPs).

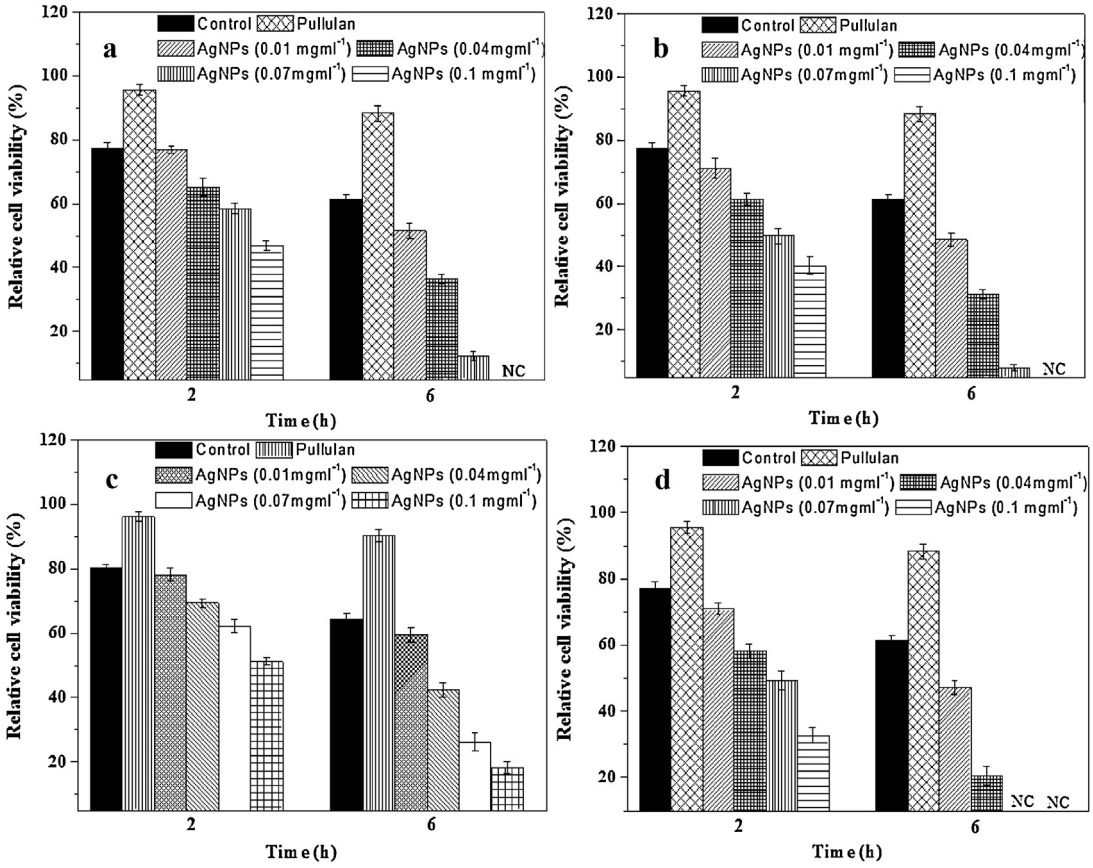

Fig. 5. Effect of AgNPs on the killing of various bacterial pathogens such as *E. coli* (a), *K. pneumonia* (b), *L. monocytogenes* (c) and *P. aeruginosa* (d) in liquid medium after 2 and 6 h of incubation at 37 °C. Both pullulan and silver nitrate were used as controls. The values are represented as mean ± S.D. NC illustrates the absence of bacterial cells.

interaction of biocide AgNPs with cell membrane leads to a loss of membrane integrity and increases leakage of intracellular ions such as K^+ and finally cell death. Similarly, Lok et al. (2006) reported the complete lose of intracellular K^+ in cells of *E. coli* during exposure to AgNPs.

3.5. Effect of AgNPs on biofilm formation

The antibiofilm activity of pullulan-stabilized AgNPs was tested against various pathogenic bacteria in 96 wells microtiter plate. Fig. 6 shows the effect of AgNPs on biofilm formation by pathogenic bacteria such as *E. coli*, *B. cereus*, *L. monocytogenes*, and *P. aeruginosa* after 24 h incubation at 37 °C. Formations of biofilms by the bacterial strains were inhibited by dose dependant manner. Decreases in biofilm formation were observed with increasing addition of AgNPs. Silver nanoparticles was completely inhibited the formation of biofilms by *E. coli* and the multidrug resistant pathogen *P. aeruginosa* at 28 and 52 μg/ml, respectively. These results are in good agreement with results obtained by Radzig et al. (2013) who found that biofilm formation by *P. aeruginosa* and *E. coli* decreased when the concentration of silver nanoparticles was increased from 0.125 μg/ml to 16 μg/ml. This biofilm inhibition was dependent on the size of the AgNPs. Kora and Arunachalam (2011) reported that the lowest concentration of AgNPs (1 μg/ml) was found to be inhibited >95% biofilm formation by *P. aeruginosa*. This inhibition may have been due to the direct interaction of AgNPs with bacterial cells without aggregation. The silver nanoparticles (100 nM) effectively inhibited biofilm formation by *P. aeruginosa* and *S. epidermidis* with respective values of 95% and 98% which could be due to the induction of bacterial cell detachment during biofilm formation (Kalishwaralal et al., 2010).

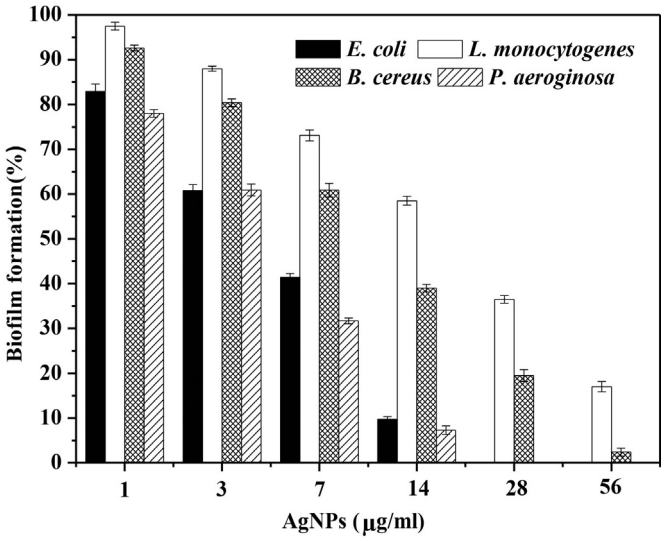

Fig. 6. Effect of AgNPs on the inhibition of biofilm formation by *E. coli*, *L. monocytogenes*, *B. cereus* and *P. aeruginosa*. The values are represented as mean ± S.D.

4. Conclusions

Synthesis of pullulan-mediated AgNPs was developed using a very safe, simple, cost effective, and energy saving method. The synthesized AgNPs was first confirmed by UV–vis spectroscopy followed by TEM, EDX, DLS, XRD, and FT-IR measurements. The pullulan-reduced AgNPs were stable for up to 3 months at room

temperature and their potent antibacterial and antibiofilm activities were analyzed using the agar well diffusion and *in vitro* killing method against food-born and multidrug resistant pathogens such as *E. coli*, *L. monocyogenes*, *B. cereus*, *K. pneumonia*, and *P. aeruginosa*. Moreover, antifungal activity was evaluated against fungal pathogens such as *Aspergillus* spp., and *Penicillum* spp. Results of antimicrobial activity revealed that the all bacterial and fungal pathogens were inhibited in a dose-dependent manner. The pathogen *P. aeruginosa* was more susceptible to AgNPs followed by *K. pneumonia* and *E. coli*. These experimental results suggest that pullulan-reduced AgNPs can be used as potent antimicrobial agent for various biomedical applications.

Acknowledgement

The authors gratefully acknowledge the Brain Korea 21 (BK21) program, Government of South Korea for their financial support.

References

Bankura, K. P., Maity, D., Mollick, M. M. R., Mondal, D., Bhowmick, B., Bain, M. K., et al. (2012). Synthesis, characterization and antimicrobial activity of dextran stabilized silver nanoparticles in aqueous medium. *Carbohydrate Polymers*, *89*, 1159–1165.

Bindhu, M. R., & Umadevi, M. (2013). Synthesis of monodispersed silver nanoparticles using *Hibiscus cannabinus* leaf extract and its antimicrobial activity. *Spectrochimica Acta part A: Molecular and Biomolecular Spectrocopy*, *101*, 184–190.

Duncan, T. V. (2011). Applications of nanotechnology in food packaging and food safety: Barrier materials, antimicrobials and sensors. *Journal of Colloid and Interface Science*, *363*, 1–24.

Gajbhiye, M., Kesharwani, J., Ingle, A., Gade, A., & Rai, M. (2009). Fungus-mediated synthesis of silver nanoparticles and their activity against pathogenic fungi in combination with fluconazole. *Nanomedicine: Nanotechnology, Biology and Medicine*, *5*, 382–386.

Gan, P. P., Ng, S. H., Huang, Y., & Yau Li, S. F. (2012). Green synthesis of gold nanoparticles using palm oil mill effluent (POME): A low-cost and eco-friendly viable approach. *Bioresource Technology*, *113*, 132–135.

Guari, Y., Thieuleux, C., Mehdi, A., Reye, C., Corriu, R. J. P., Gomez-Gallardo, S., et al. (2003). In situ formation of gold nanoparticles within thiol functionalized HMS-C-16 and SBA-15 type materials via an organometallic two-step approach. *Chemistry of Materials*, *15*, 2017–2024.

Hebeish, A., Hashem, M., Abd El-Hady, M. M., & Sharaf, S. (2013). Development of CMC hydrogels loaded with silver nano-particles for medical applications. *Carbohydrate Polymers*, *92*, 407–413.

Jung, S. W., Jeong, J. I., & Kim, S. H. (2003). Characterization of hydrophobized pullulan with various hydrophobicities. *International Journal of Pharmaceutics*, *254*, 109–121.

Kalishwaralal, K., BarathManiKanth, S., Ram Kumar Pandian, S., Deepak, V., & Gurunathan, S. (2010). Silver nanoparticles impede the biofilm formation by *Pseudomonas aeruginosa* and *Staphylococcus epidermidis*. *Colloids and Surfaces B: Biointerfaces*, *79*, 340–344.

Kora, A. J., & Arunachalam, J. (2011). Assessment of antibacterial activity of silver nanoparticles on *Pseudomonas aeruginosa* and its mechanism of action. *World Journal of Microbiology and Biotechnology*, *27*, 1209–1216.

Lok, C. N., Ho, C. M., Chen, R., He, Q. Y., Yu, W. Y., & Sun, H. (2006). Proteomic analysis of the mode of antibacterial action of silver nanoparticles. *Journal of Proteome Research*, *5*, 916–924.

Magudapatty, G., Gangopaghyayrans, P., Panigrahi, B. K., Nair, K. G. M., & Dhara, S. (2001). Electrical transport studies of Ag nanoparticles embedded in glass matrix. *Physica B: Condensed Matter*, *299*, 142–146.

Mohanty, S., Mishra, S., Jena, P., Jacob, B., Sarkar, B., & Sonawane, A. (2012). An investigation on the antibacterial, cytotoxic, and antibiofilm efficacy of starch-stabilized silver nanoparticles. *Nanomedicine: Nanotechnology, Biology and Medicine*, *8*, 916–924.

Mona, G., & Ajay Kumar, G. (2004). In vitro cytotoxicity studies of hydrogel pullulan nanoparticles prepared by AOT/N-hexane micellar system. *Journal of Pharmacy and Pharmaceutical Science*, *7*, 38–46.

Moura, M. R. de, Mattoso, L. H. C., & Zucolotto, V. (2012). Development of cellulose-based bactericidal nanocomposites containing silver nanoparticles and their use as active food packaging. *Journal Food Engineering*, *109*, 520–524.

Narayanan, K. B., & Sakthivel, N. (2011). Heterogeneous catalytic reduction of anthropogenic pollutant, 4-nitrophenolby silver-bionanocomposite using *Cylindrocladium floridanum*. *Bioresource Technology*, *102*, 10737–10740.

Pandey, S., Goswami, G. K., & Nanda, K. K. (2012). Green synthesis of biopolymer–silver nanoparticle nanocomposite: An optical sensor for ammonia detection. *International Journal of Biological Macromolecules*, *51*, 583–589.

Peng, H., Yang, A., & Xiong, J. (2013). Green, microwave-assisted synthesis of silver nanoparticles using bamboo hemicelluloses and glucose in an aqueous medium. *Carbohydrate Polymers*, *91*, 348–355.

Pol, V. G., Srivastava, D. N., Palchik, V., Slifkin, M. A., Weiss, A. M., & Gedanken, A. (2002). Sonochemical deposition of silver nanoparticles on silica spheres. *Langmuir*, *18*, 3352–3357.

Priyadarshini, S., Gopinath, V., Meera Priyadharsshini, N., MubarakAli, D., & Velusamy, P. (2013). Synthesis of anisotropic silver nanoparticles using novel strain, *Bacillus flexus* and its biomedical application. *Colloids and Surfaces B: Biointerfaces*, *102*, 232–237.

Radzig, M. A., Nadtochenko, V. A., Koksharova, O. A., Kiwi, J., Lipasova, V. A., & Khmel, I. A. (2013). Antibacterial effects of silver nanoparticles on gram-negative bacteria: Influence on the growth and biofilms formation, mechanisms of action. *Colloids and Surfaces B: Biointerfaces*, *102*, 300–306.

Roopan, S. M., Rohit Madhumitha, G., Abdul Rahumanb, A., Kmaraj, C., Bharathi, A., & Surendra, T. V. (2013). Low-cost and eco-friendly phyto-synthesis of silver nanoparticles using *Cocos nucifera* coir extract and its larvicidal activity. *Industrial Crops and Products*, *43*, 631–635.

Sharma, V. K., Yngard, R. A., & Lin, Y. (2009). Silver nanoparticles: Green synthesis and their antimicrobial activities. *Advances in Colloid and Interface Science*, *145*, 83–96.

Shukla, M. K., Singh, R. P., Reddy, C. R. K., & Jha, B. (2012). Synthesis and characterization of agar-based silver nanoparticles and nanocomposite film with antibacterial applications. *Bioresource Technology*, *107*, 295–300.

Stiger, R. M., Gorer, S., Craft, B., & Penner, P. M. (1999). Investigations of electrochemical silver nanocrystal growth on hydrogen-terminated silicon (1 0 0). *Langmuir*, *15*(3), 790–798.

Wei, X., Luo, M., Li, W., Yang, L., Liang, X., Xu, L., et al. (2012). Synthesis of silver nanoparticles by solar irradiation of cell-free *Bacillus amyloliquefaciens* extracts and $AgNO_3$. *Bioresource Technology*, *103*, 273–278.

Wu, J., Zhong, F., Li, Y., Shoemaker, F. F., & Xia, W. (2013). Preparation and characterization of pullulan-chitosan and pullulan-carboxymethyl chitosan blended films. *Food Hydrocolloids*, *30*, 82–91.

Yoksan, R., & Chirachanchai, S. (2010). Silver nanoparticle-loaded chitosan–starch based films: Fabrication and evaluation oftensile, barrier and antimicrobial properties. *Materials Science and Engineering C*, *30*, 891–897.

Zhu, J. J., Liu, S. W., Palchik, O., Kottypin, Y., & Gedanken, A. (2000). Shape-controlled synthesis of silver nanoparticles by pulse sonoelectrochemical methods. *Langmuir*, *16*, 6396–6399.